EPJ Web of Conferences **61**, 01007 (2013)
DOI: 10.1051/epjconf/ 20136101007

The force-free magnetosphere of a rotating black hole

Ioannis Contopoulos[1,a]

[1] *Research Center for Astronomy and Applied Mathematics, Academy of Athens, Athens 11527, Greece*

Abstract. We explore the analogy with pulsars and investigate the structure of the force-free magnetosphere around a Kerr black hole. We propose that the source of the black hole magnetic field is the Poynting-Robertson effect on the plasma electrons at the inner edge of the surrounding accretion disk, the so called Cosmic Battery. The magnetospheric solution is characterized by the distributions of the magnetic field angular velocity and the poloidal electric current. These are not arbitrary. They are determined self-consistently by requiring that magnetic field lines cross smoothly the two singular surfaces of the problem, the inner 'light surface' located inside the ergosphere, and the outer 'light surface' which is the generalization of the pulsar light cylinder. The black hole forms a relativistic jet only if it is surrounded by a thick disk and/or extended disk outflows.

1 The analogy with pulsars

The electromagnetic extraction of energy from a spinning black hole can be one of the most powerful and efficient engines in the Universe. [2] first argued that a spinning black hole threaded by a sufficiently strong magnetic field and permeated by an electron-positron plasma generated from pair cascades establishes a force-free magnetosphere, in direct analogy to the theory of 'pulsar electrodynamics' developed a few years earlier by [15]. [21] realized that *many astrophysicists feel uncomfortable in curved space-time* (sic) and rewrote black hole electrodynamics in an absolute-space/universal-time formulation *with the hope that it may catalyze pulsar-experienced astrophysicists to begin research in black hole electrodynamics and to bring to bear on this topic their lore about the axisymmetric pulsar problem* (sic). Unfortunately, all these years, black hole magnetospheres did not attract the same level of attention as pulsar theory.

We decided to explore the analogy with pulsars even further. The structure of the ideal force-free axisymmetric pulsar magnetosphere was obtained for the first time in [10]. Since then, we have moved on to the investigation of non-ideal pulsar magnetospheres with various prescriptions for the finite plasma conductivity ([16], [19]). The main elements of the pulsar magnetosphere (pm) are the following:

1pm: The neutron star magnetic field is generated by electric currents in its interior. In particular, an isolated neutron star supports its own magnetic field.

2pm: The magnetosphere contains a region of closed field lines that corotate with the central neutron star. That region extends out to the 'light cylinder' where if a particle were to corotate with the star, it would do so at the speed of light.

3pm: Magnetic field lines that cross the light cylinder open up to infinity in a 'backward wound' monopole configuration.

4pm: A central element of the magnetosphere is the poloidal current sheet that takes care of magnetospheric current closure. It extends from the tip of the closed line region on the light cylinder to infinity, and from the tip to the surface of the star along the separatrix between closed and open field lines.

5pm: Electrons and positrons are freely supplied in the magnetosphere through high energy pair production processes at the positions where magnetic field lines cross the surface of zero spatial charge. These are the outer gaps ([24]) and the tip of the closed line region ([5]).

6pm: The neutron star loses energy in the form of electromagnetic (Poynting) energy at a rate proportional to the square of the total amount of open magnetic flux and to the square of the rotation angular velocity.

Carrying over the above to the black hole (bh) case we see the following analogies/differences:

1bh: A Kerr black hole cannot support its own magnetic field. A magnetic field can thread the black hole horizon only if it is generated or advected in a surrounding accretion disk. Even so, a Kerr black hole repels the magnetic field from its horizon (the repulsion is complete for a maximally rotating hole), unless either the accretion disk extends down to the horizon, or the black hole becomes charged ([29]).

2bh: A Kerr black hole does not contain a closed line region. Moreover, the absence of a perfectly conducting surface does not allow it to impose corotation at the angular velocity of the black hole. Still, the field lines isorotation law applies in ideal black hole magnetospheres too, and a generalized light cylinder still forms.

[a] e-mail: icontop@academyofathens.gr

3bh: Magnetic field lines that cross the generalized light cylinder are expected to open up to infinity in a 'backward wound' monopole configuration similar to pulsars.

4bh: The magnetosphere is expected to also contain a poloidal current sheet that takes care of magnetospheric current closure.

5bh: Electrons and positrons are freely supplied in outer magnetospheric gaps.

6bh: The black hole is expected to lose energy at a rate proportional to the square of the total amount of open magnetic flux and to the square of the field line rotation angular velocity. The latter is found to be close to the black hole angular velocity.

Before we proceed with a numerical solution for the black hole magnetosphere, we would like to discuss what is the origin of the black hole magnetic field.

2 The Cosmic Battery

It is a common belief in the astrophysics community that black hole jets are associated with large scale magnetic fields that thread the horizon and/or the ergosphere. A Kerr black hole cannot support such fields in vacuum, therefore, an astrophysical black hole must be surrounded by an accretion disk that holds the magnetic field in place. Without the disk, any magnetic field that happens to thread the black hole horizon will escape within light crossing times.

The origin of the accretion disk magnetic field is not well established. One school of thought assumes that the field is carried in from large distances ([3], [27]). However, astrophysical accretion disks are known to be turbulent due to the magneto-rotational instability. As a result, they are both viscous and diffusive. In fact, magnetic field diffusion is so strong that it is more natural for magnetic flux to escape outward than to accumulate inward ([7]). Therefore, the inward advection of magnetic flux is currently an open issue. Even if the presence of a large scale organized magnetic field in the innermost region of the accretion disk is guaranteed, we do not yet understand why some systems show large scale jets and others do not (e.g. the radio loud/radio quiet dichotomy in AGNs, the formation/disruption of jets in X-ray binaries, etc.). Moreover, observationally, there seems to be no relation between the power in the jet and the black hole spin ([13]), and yet, theoretically, the two are related.

One way to address all of the above issues is to propose that the necessary large scale magnetic field is generated in-situ by the Cosmic Battery ([7], [9]), and that under certain conditions the mechanism becomes very efficient, whereas under different conditions it becomes inefficient ([18]). This astrophysical mechanism is based on the Poynting-Robertson drag effect on the electrons of the innermost plasma orbiting a black hole or neutron star, and has found observational support in observations of the Faraday rotation-measure gradients across extragalactic jets ([6], [4]). We will now show how the Cosmic Battery works in a stellar-mass black hole X-ray binary. Our results can be directly generalized in a supermassive black hole AGN.

It is well known that the accretion disk around a black hole does not extend all the way to the event horizon, but is truncated at an inner radius due to the existence of an innermost stable circular orbit (hereafter ISCO). As the accretion disk material gradually spirals in towards the ISCO, it emits blackbody radiation with higher and higher temperature reaching $\sim 10^7$ K at the ISCO. Inside that radius, the material is essentially in free fall and emits very little radiation.

Electrons in the plasma orbiting the black hole at the inner edge of the accretion disk scatter photons coming from the opposite side of the inner edge of the disk. As they are circling the black hole, they see the photons aberrated as coming slightly from the head-on direction. Thus, they experience a force against their direction of motion[1]. The ions feel a much smaller radiation-drag force than the electrons because their Thompson cross section is inversely proportional to the square of the mass of the scatterer. This difference in the radiation-drag force leads to *a growing relative motion between electrons and ions equivalent to an increasing electric current in the direction of rotation, and therefore to a growing axial magnetic field.* When one goes beyond the MHD treatment and incorporates the equations of motion of the electrons and ions one sees that, the growth of the axial magnetic field is associated with an azimuthal electromotive field $E_{\rm CB}$ in the direction opposite to that of rotation at the inner edge of the accretion flow ([7]). There is little or no azimuthal electromotive field inside the ISCO (the plasma freely plunges in) or at larger radii in the accretion disk (the optical depth increases and the radiation flux decreases rapidly with distance). *The growth of the axial magnetic field around the inner edge of the accretion flow is driven by the non-zero curl of the distribution of azimuthal electromotive field* $E_{\rm CB}$ according to the induction equation:

$$\frac{\partial B}{\partial t} = -c\nabla \times E_{\rm CB} = -\frac{c}{r}\frac{\partial}{\partial r}(rE_{\rm CB})\,. \qquad (1)$$

Note that advection and diffusion have been ignored here in order to simplify the presentation. The magnetic field can grow up to a maximum value dictated by equipartition with the kinetic energy of the plasma at the inner edge of the accretion disk. The following estimates are obtained for a non-rotating Schwarzchild black hole and can be directly generalized in the case of a rotating Kerr black hole. The inner edge of the disk is assumed to lie at the position of the ISCO, namely at $r = 6GM/c^2 \sim 10(M/M_\odot)$km. At this position, we can estimate the equipartition magnetic field as

$$\begin{aligned} B_{eq} &\sim (4\pi\rho v_r v_K)^{1/2} \sim \left(\frac{2\dot{M}v_K}{rh}\right)^{1/2} \\ &\sim 10^8\,\dot{m}^{1/2}\left(\frac{h}{r}\right)^{-1/2}\left(\frac{M}{M_\odot}\right)^{-1/2}\ {\rm G}\,, \end{aligned} \qquad (2)$$

where ρ is the density, v_r and v_K are the radial and the Keplerian velocities, respectively, and $\dot{m}$ is the mass accretion

[1] The aberration of radiation is the essence of the Poynting-Robertson effect felt by grains in orbit around the Sun. [7] applied the same principle on the electrons in a plasma orbiting an astrophysical compact object, assuming an isotropic source of radiation at the center.

rate in units of its Eddington value $\dot{M}_E \equiv L_E/c^2$. Here all quantities have been evaluated at the ISCO. At early times, eq. (1) applies continuously, and the growth of the magnetic field is linear with a characteristic timescale τ_{eq} to reach equipartition equal to

$$\tau_{eq} \sim \frac{rB_{eq}}{2cE_{PR}} . \quad (3)$$

In order to complete our calculation, we need to estimate the electromotive field $E_{\rm CB}$. Such a calculation requires a detailed consideration of photon orbits in the relativistic environment of a black hole. Here we estimate this term geometrically from the radiation that an electron at the ISCO sees as coming from the 'wall' of height h at the opposite side of the inner edge of the accretion flow. The total luminosity that reaches the electron at $\sim 90^\circ$ to its motion can be estimated as

$$L \sim f\sigma T^4 \pi r h \sim 10^{36}\, f\, T_7^4 \left(\frac{M}{M_\odot}\right)^2 \left(\frac{h}{r}\right) \text{ erg s}^{-1} , \quad (4)$$

where T_7 is the ISCO equivallent blackbody temperature in units of 10^7 K, σ is the Stefan-Boltzmann constant, and the geometric factor f of order unity is due to the fact that part of the radiation coming from the opposite side of the flow is falling into the black hole and not reaching the other side. The Cosmic Battery electromotive field can now be estimated as

$$E_{\rm CB} \sim g \frac{L\sigma_T}{4\pi r^2 ce} \frac{v_K}{c} , \quad (5)$$

where σ_T is the electron Thomson cross-section, v_K/c is the Poynting-Robertson aberration effect due to the photons 'hitting' the moving electrons on the other side at about 90°, and g is a geometric factor of order unity. Putting everything back together in eq. (3) we obtain

$$\tau_{eq} \sim 4\times 10^5 (fg)^{-1} T_7^{-4} \dot{m}^{1/2} \left(\frac{h}{r}\right)^{-3/2} \left(\frac{M}{M_\odot}\right)^{1/2} \text{ s.} \quad (6)$$

In order to reach a current strong enough to produce a magnetic field on the order of 10^6 G ($\sim$ 10% of the equipartition value) required to explain the radio emission in a $10M_\odot$ source like Cyg X-1 ([14]), the battery must operate for about 12 hours, if the inner part of the accretion flow is described by an ADAF with $h/r \sim 1$ and $\dot{m} \sim 10^{-1}$. This timescale is short compared to the system evolution timescale in the hard state. On the other hand, when the system transits from the hard to the soft state, the accretion flow changes from a thick ADAF to a Shakura-Sunyaev thin disk with $h/r \sim 10^{-1}$. In that case, the timescale for the growth of a 10^6 G magnetic field ($\sim$ 3% of the equipartition value) becomes of the order of 5 days (assuming $\dot{m}$ is still $\sim 10^{-1}$), which is longer than the characteristic evolution timescale of the black-hole X-ray binary in the soft state (as an example, see the 300-day outburst of J1752-223 in [26]).

3 Solutions of the GR pulsar equation

We have shown that the inner accretion disk can generate and accumulate a certain amount Ψ_{max} of magnetic flux around the central rotating Kerr black hole. In order to study the resulting force-free magnetosphere we follow the 3+1 formulation of [21] used by most researchers in the astrophysical community. We restrict our analysis to steady-state and axisymmetric space times where $(\ldots)_{,t} = (\ldots)_{,\phi} = 0$. In that case, the general 4-dimensional space-time geometry may be written in Boyer-Lindquist spherical coordinates $x^\mu \equiv (t, r, \theta, \phi)$ as

$$ds^2 = -\alpha^2 dt^2 + \frac{A\sin^2\theta}{\Sigma}(d\phi - \Omega dt)^2 + \frac{\Sigma}{\Delta}dr^2 + \Sigma d\theta^2 . \quad (7)$$

Here, $\alpha \equiv (\Delta\Sigma/A)^{1/2}$ and $\Omega \equiv 2aMr/A$ are the lapse function and angular velocity of 'zero-angular momentum' fiducial observers (ZAMOs) respectively,

$$\Delta \equiv r^2 - 2Mr + a^2 \ , \ \Sigma \equiv r^2 + a^2\cos^2\theta \ ,$$

$$A \equiv (r^2+a^2)^2 - a^2\Delta\sin^2\theta ,$$

M is the black hole mass, and a its angular momentum ($0 \le a \le M$). The fundamental equation that governs the steady-state structure of the force-free magnetosphere around a Kerr black hole becomes

$$\rho_e E + J \times B = 0 . \quad (8)$$

Here, E, B are the electric and magnetic fields measured by ZAMOs; ρ_e and J are the electric charge and current densities. Eq. (8) is supplemented by Maxwell's equations of electrodynamics in curved spacetime

$$\begin{aligned} \nabla\cdot B &= 0 \\ \nabla\cdot E &= 4\pi\rho_e \\ \nabla\times(\alpha B) &= 4\pi\alpha J \\ \nabla\times(\alpha E) &= 0 . \end{aligned} \quad (9)$$

For several applications in astrophysics, perfect (infinite) conductivity is a valid approximation. In this case,

$$E\cdot B = 0 , \quad (10)$$

and the electric and magnetic vector fields can be expressed in terms of three scalar functions, $\Psi(r,\theta)$, $\omega(\Psi)$, and $I(\Psi)$ as

$$B(r,\theta) = \frac{1}{2\pi\sqrt{A}\sin\theta}\left\{\Psi_{,\theta}, -\sqrt{\Delta}\Psi_{,r}, \frac{2I\sqrt{\Sigma}}{\alpha}\right\} \quad (11)$$

$$E(r,\theta) = \frac{\Omega-\omega}{2\pi\alpha\sqrt{\Sigma}}\left\{\sqrt{\Delta}\Psi_{,r}, \Psi_{,\theta}, 0\right\} . \quad (12)$$

ω is the angular velocity of the magnetic field lines, I is the poloidal electric current flowing through the circular loop r =const., θ =const., and Ψ is the total magnetic flux enclosed in that loop. Notice that the electric field changes sign close to the horizon with respect to its sign

at large distances. As explained in [2], a rotating observer (ZAMO) will in general see a Poynting flux of energy *entering* the horizon, but he will also see a sufficiently strong flux of angular momentum *leaving* the horizon. That ensures that energy is extracted from the black hole. The poloidal component of Eq. (8) then yields the general relativistic force-free Grad-Shafranov equation

$$\left\{\Psi_{,rr}+\frac{1}{\Delta}\Psi_{,\theta\theta}+\Psi_{,r}\left(\frac{A_{,r}}{A}-\frac{\Sigma_{,r}}{\Sigma}\right)-\frac{\Psi_{,\theta}}{\Delta}\frac{\cos\theta}{\sin\theta}\right\}$$
$$\cdot\left[1-\frac{\omega^2 A\sin^2\theta}{\Sigma}+\frac{4M\alpha\omega r\sin^2\theta}{\Sigma}-\frac{2Mr}{\Sigma}\right]$$
$$-\left(\frac{A_{,r}}{A}-\frac{\Sigma_{,r}}{\Sigma}\right)\Psi_{,r}-\left(2\frac{\cos\theta}{\sin\theta}-\frac{A_{,\theta}}{A}+\frac{\Sigma_{,\theta}}{\Sigma}\right)$$
$$\cdot(\omega^2 A\sin^2\theta-4M\alpha\omega r\sin^2\theta+2Mr)\frac{\Psi_{,\theta}}{\Delta\Sigma}$$
$$+\frac{2Mr}{\Sigma}\left(\frac{A_{,r}}{A}-\frac{1}{r}\right)\Psi_{,r}+\frac{4\omega M\alpha r\sin^2\theta}{\Sigma}$$
$$\cdot\left\{\Psi_{,r}\left(\frac{1}{r}-\frac{A_{,r}}{A}\right)-\frac{\Psi_{,\theta}}{\Delta}\frac{A_{,\theta}}{A}\right\}$$
$$-\frac{\omega'\sin^2\theta}{2\pi\Sigma}(\omega A-2\alpha Mr)\left(\Psi_{,r}^2+\frac{1}{\Delta}\Psi_{,\theta}^2\right)$$
$$=-\frac{4\Sigma}{\Delta}II' \qquad (13)$$

(Eq. (3.14) of [2] re-written in our notation). Primes denote differentiation with respect to Ψ. One sees directly that if we set $\alpha = 0$, $M = 0$, and ω equal to the neutron star angular velocity in eq. (13) we obtain

$$\left(\Psi_{,rr}+\frac{1}{r^2}\Psi_{,\theta\theta}+\frac{2\Psi_{,r}}{r}-\frac{1}{r^2}\frac{\cos\theta}{\sin\theta}\Psi_{,\theta}\right)\cdot[1-\omega^2 r^2\sin^2\theta]$$
$$-\frac{2\Psi_{,r}}{r}-2\omega^2\cos\theta\sin\theta\Psi_{,\theta}=-4II' \,, \qquad (14)$$

which is the well known pulsar equation ([25]). The zeroing of the term multiplying the second order derivatives in eq. (13),

$$1-\frac{\omega^2 A\sin^2\theta}{\Sigma}+\frac{4M\alpha\omega r\sin^2\theta}{\Sigma}-\frac{2Mr}{\Sigma}=0 \,, \qquad (15)$$

yields the singular surfaces of the problem, the so called *'light surfaces'* (LS)[2]. When we set $M = \alpha = 0$, it yields the standard pulsar light cylinder $r\sin\theta = c/\omega$. In general, the shape of the outer LS is only asymptotically cylindrical as $\theta \to 0$ (see figure 3 below), and an inner LS appears inside the ergosphere. It is interesting to note that the outer boundary of the ergosphere corresponds to the solution of the singularity condition for $\omega = 0$, whereas the inner boundary (the event horizon at $r = r_{\rm BH} \equiv M + \sqrt{M^2 - a^2}$) corresponds to the solution of the singularity condition for $\omega = \Omega_{\rm BH} \equiv a/(r_{\rm BH}^2 + a^2)$, where $\Omega_{\rm BH}$ is the angular velocity of the black hole. It is also interesting to note that the natural 'radiation condition' at infinity (energy must flow outwards along all field lines) requires that

$$0 \le \omega \le \Omega_{\rm BH} \,, \qquad (16)$$

and therefore indeed the inner LS lies inside the ergosphere ([2]).

Both Eqs. (13) and (14) contain the two functions, $\omega(\Psi)$ and $I(\Psi)$, which must be determined by the physics of the problem. In the case of an axisymmetric spinning neutron star, ω is usually taken to be equal to the neutron star angular velocity. In pulsars, $I(\Psi)$ is self-consistently determined through an iterative numerical technique that implements a smooth crossing of the light cylinder where $r\sin\theta = c/\omega$ ([10], [28]). In the case of a spinning black hole, the situation is qualitatively similar but more complicated. Contrary to a neutron star, the black hole does not have a solid surface, and therefore it cannot impose any restriction on ω other than the 'radiation condition' Eq. (16). The only natural restriction that is imposed by the physical problem is that magnetic field lines must be smooth and continuous everywhere. $\omega(\Psi)$ must therefore be determined together with $I(\Psi)$ through the condition of smooth crossing of both LS of the problem, the inner one inside the ergosphere, and the outer one at large distances. This can be achieved through an iterative numerical technique analogous to the one employed in the pulsar magnetosphere (see [10] and [11] for details). As remarked previously, iterating with respect to two functions simultaneously is indeed a very difficult task.

The results of our numerical integration are shown in figures 1-4. We show here the magnetic field configuration for a maximally rotating black hole ($a = M$) near the black hole horizon (figure 1) and at larger distances (left panel of figure 3). We also plot (red lines in figures 1 and 3) the inner LS inside the ergosphere, and the outer LS which becomes asymptotically cylindrical as $\theta \to 0$. Notice that magnetic field lines are monopolar at large distances (beyond a few times the radius of the event horizon), and they bend upwards towards the axis as they approach the horizon. In figure 2 we show the distributions of $\omega(\Psi)$ (left panel), and $2|I(\Psi)|$ (right panel), for six values of the black hole spin parameter a for the case shown in figure 1. $\omega(\Psi)$ is equal to $0.5\Omega_{\rm BH}$ to within 10%, and $I(\Psi)$ is very close to the analytical expression for a split monopole ([22]), also to within 10%. As is the case in pulsars, the magnetospheric electric current is non-zero at $\Psi = \Psi_{max}$, and the global electric circuit closes through an equatorial current sheet (green lines in figures 1 and 3).

4 Black hole jets and winds

We believe that the study of the steady-state open force-free black hole magnetosphere offers a deeper insight than time-dependent numerical simulations. In analogy to the axisymmetric force-free pulsar magnetosphere, we argued that steady-state solutions can only be obtained through a self-consistent determination of the distributions of both the magnetic field angular velocity and the magnetospheric electric current $\omega(\Psi)$ and $I(\Psi)$ respectively.

[2]These are none other than the *'velocity-of-light surfaces'* of [20] where the speed relative to the ZAMOs of a particle moving purely toroidally with angular velocity ω equals c.

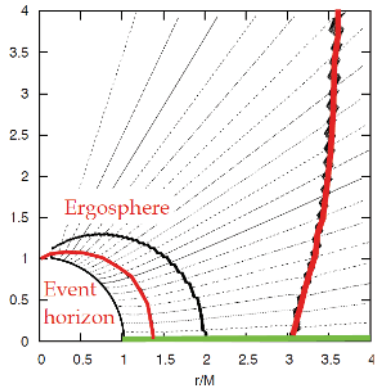

Figure 1. The inner magnetosphere of a maximally rotating black hole surrounded by a thin disk. Thick lines from the center outwards respectively: the event horizon, the inner LS (red), the outer boundary of the ergosphere, and the outer LS (red). Green line: current sheet.

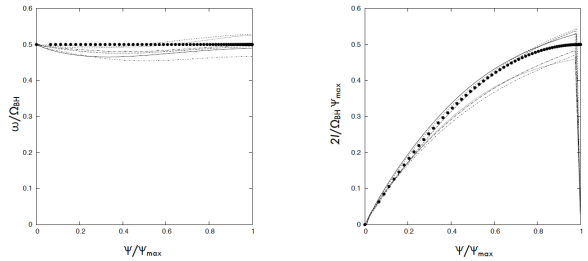

Figure 2. Distributions of $\omega(\Psi)$ normalized to $\Omega_{\rm BH}$ (left panel), and $2|I(\Psi)|$ normalized to $\Omega_{\rm BH}\Psi_{max}$ (right panel) for various values of the black hole spin parameter a/M. All three distributions are close to the analytical split monopole expressions (thick dots).

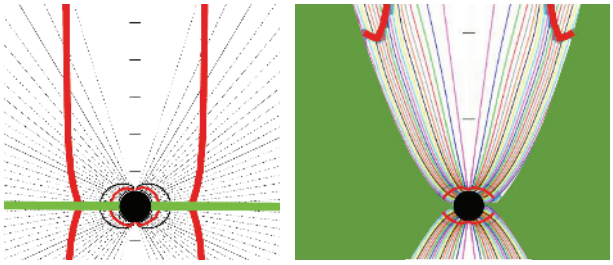

Figure 3. Magnetospheres of a maximally rotating black hole surrounded by a thin disk (left panel) and a thick disk-wind (right panel). Colors as in figure 1. In both cases, a current sheet forms along the last open field line that threads the horizon.

These can only be determined when open field lines cross both singular LS, the inner LS inside the ergosphere outside the black hole horizon, and the outer LS which is a deformed light cylinder. All field lines that cross the black hole horizon are bound to cross the inner LS. This is not the case, though, for the outer LS. In fact, several numerical simulations exist in the literature where the black hole is threaded by a vertical uniform magnetic field, and yet

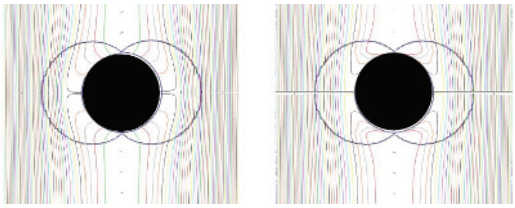

Figure 4. Non-uniqueness of solutions with an externally imposed vertical background field. Field lines cross only the inner light surface (not the outer one), and therefore one can freely specify $I(\Psi)$ and numerically obtain $\omega(\Psi)$. As in figure 3, these solutions too contain a current sheet along the last open field line that threads the horizon.

they converge to certain distributions of $\omega(\Psi)$ and $I(\Psi)$ (e.g. [17], [23]). In that case, the steady-state solution is mathematically indeterminate, and indeed, when we freely specify one of the two free functions, e.g. $I(\Psi)$, we obtain different solutions for $\omega(Psi)$ as shown in figure 4.

In summary, the force-free spinning black hole magnetosphere is not very different from the asymptotic force-free axisymmetric pulsar magnetosphere. Black holes surrounded by thin accretion disks generate a radial relativistic wind that carries electromagnetic (Poynting) flux. In fact, beyond a distance on the order of a few times the black hole radius, the two problems are almost identical. It is interesting to note here, again similarly to pulsars, that beyond the light cylinder *the Lorentz factor* Γ *in the radial wind increases linearly with cylindrical distance* as

$$\Gamma \propto \frac{r\sin\theta}{c/\omega} \approx \frac{r\Omega_{\rm BH}\sin\theta}{2c} \qquad (17)$$

([8]), possibly up to the fast magnetosonic point of the outflow. Therefore, according to Eq. (17), field/flow lines that extend further away from the axis are expected to reach higher Lorentz factors. Of course, the final Lorentz factor will also depend on the mass loading of a given magnetic field line.

We conclude that the black hole + disk system cannot account for the origin of black hole relativistic jets. Notice that the artificial imposition of an external vertical background field does not really solve the collimation problem. A more plausible situation is one that includes an MHD disk wind. We know ([1], [12]) that such winds are collimated, and therefore they may provide a natural outer boundary for the collimation of the relativistic black hole wind, as shown in the right panel of figure 3. In that case, the numerical iteration between the two light surfaces yields a different solution for $\omega(\Psi)$ and $I(\Psi)$, in direct agreement with the results of the time-dependent force-free general relativistic simulations of [27]. We plan to continue in the future our investigation of the interrelation between the black hole, the accretion disk, and the disk outflows.

We would like to thank Dave Meier for his comments on our presentation. This work was supported by the General Secretariat for Research and Technology of Greece and the European Social Fund in the framework of Action 'Excellence'.

References

[1] Blandford, R. D. & Payne, D. G., MNRAS, **199**, 883 (1982)

[2] Blandford, R. D. & Znajek, R. L., MNRAS, **179**, 433 (1977)

[3] Cao, X. & Spruit, H. C., ApJ, **765** 149 (2013)

[4] Christodoulou, D. M., Gabuzda, D. C., Contopoulos, I., & Kazanas, D., A&A, submitted (2013)

[5] Contopoulos, I., A& A, **442**, 579 (2005)

[6] Contopoulos, I., Christodoulou, D. M., Kazanas, D., & Gabuzda, D. C., ApJ, 702, L148 (2009)

[7] Contopoulos, I. & Kazanas, D., ApJ, **508**, 859 (1998)

[8] Contopoulos, I. & Kazanas, D., ApJ, **566**, 336 (2002)

[9] Contopoulos, I., Kazanas, D., & Christodoulou, D. M., ApJ, **652**, 1451 (2006)

[10] Contopoulos, I., Kazanas, D. & Fendt, C., ApJ, **511**, 351 (1999)

[11] Contopoulos, I., Kazanas, D. & Papadopoulos, D. B., ApJ, **765**, 113 (2013)

[12] Contopoulos, J., & Lovelace, R. V. E., ApJ, **429**, 139 (1994)

[13] Fender, R. P., Gallo, E. & Russell, D., MNRAS, **406**, 1425 (2010)

[14] Giannios, D., A&A, **437**, 1007 (2005)

[15] Goldreich, P. & Julian, W. H., ApJ, **157**, 869 (1969)

[16] Kalapotharakos, C., Kazanas, D., Harding, A. K. & Contopoulos, I., ApJ. **749**, 2 (2012)

[17] Komissarov, S. S. & McKinney, J. C., MNRAS, **377**, L49 (2007)

[18] Kylafis, N. D., Contopoulos, I., Kazanas, D. & Christodoulou, D. M., A& A, **538**, 5 (2012)

[19] Li, J., Spitkovsky, A. & Tchekhovskoy, A., ApJ, **746**, 60 (2012)

[20] Macdonald, D. A., MNRAS, **211**, 313 (1984)

[21] Macdonald, D. & Kip S.Thorne, K. S., MNRAS, **198**, 345 (1982)

[22] Michel, F. C., Rev. Mod. Phys., **54**, 1 (1982)

[23] Palenzuela, C., Bona, C., Lehner, L. & Reula, O., Class. Quant. Grav., **28**, 4007 (2011)

[24] Romani, R. W., ApJ, **470**, 469 (1996)

[25] Scharlemann, E. T. & Wagoner, R. V., ApJ, **182**, 951 (1973)

[26] Stiele, H., Muñoz-Darias, T., Motta, S., & Belloni, T., 25th Texas Symposium on Relativistic Astrophysics, Texas 2010, arXiv:1103.4312 (2011)

[27] Tchekhovksoy, A., Narayan, R. & McKinney, J. C., MNRAS, **418L**, 79 (2011)

[28] Timokhin, A. N., MNRAS, **368**, 1055 (2006)

[29] Wald, R. M., Phys. Rev. D, **10**, 1860 (1974)